

## **ZnO thin films implanted with Al, Sb and P: Optical, Structural and Electrical Characterization**

T. Viseu<sup>a,\*</sup>, J. Ayres de Campos<sup>a</sup>, A. G. Rolo<sup>a</sup>, T. de Lacerda-Arôso<sup>a</sup>, M.F. Cerqueira<sup>a</sup>, E. Alves<sup>b</sup>

<sup>a</sup> *Departamento de Física, Universidade do Minho, Campus de Gualtar 4710-057 Braga, Portugal*

<sup>b</sup> *Instituto Técnico Nuclear ITN, EN 10, 2686-953 Sacavém, Portugal*

In this work we report a study on the structure, optical and electrical properties of P, Sb and Al implanted ZnO thin films that had been produced by r.f. magnetron sputtering. The influence of the different replacing atoms on the structure and properties of the films has been explored. Looking for the best annealing conditions, two different annealing temperatures (300°C and 500°C) have been employed. Raman spectroscopy, X-ray photoelectron spectroscopy (XPS), X-ray diffraction, transmittance and d.c conductivity measurements have been used to characterize the samples.

X-ray diffraction and Raman scattering patterns confirm that after annealing, doped films keep a polycrystalline nature with (002) preferred orientation. These films remain very transparent and the electrical conductivity increases significantly after the 500°C annealing, reaching values of  $10.9 (\Omega\text{cm})^{-1}$  in the P-doped,  $10.33 (\Omega\text{cm})^{-1}$  in the Al-doped and  $0.56 (\Omega\text{cm})^{-1}$  in the Sb-doped samples.

*Keywords: ZnO; Ion implantation; X-ray; Raman; Optical properties.*

### **1. Introduction**

Transparent conducting oxides (TCOs) have long been a subject of various research <sup>[1-3]</sup> due to its unique physical properties and applications in commercial devices. ZnO is a

particularly interesting TCO example. Indeed, ZnO is a natural n-type semiconductor due to its intrinsic oxygen vacancies and/or interstitial zinc atoms. However, non-doped ZnO thin films are not electrically stable because of changes in the surface conductance due to oxygen chemisorptions and adsorptions<sup>[4]</sup>. To meet the demands of several application fields, ZnO may be doped with a wide variety of ions. F, B, Al, Ga, In, Sn, ..., have typically been used as dopant elements to produce conducting ZnO-based films.

The scientific community is now looking for high-quality, p-type ZnO thin films for the development of ZnO-based optoelectronic devices<sup>[5,6]</sup>. However, it is rather difficult to achieve low resistivity, high-hole-concentration conduction, deep acceptor level and low solubility of the acceptor dopants.

In this work, experimental results of Sb, Al and P-doped ZnO thin films are presented and discussed. Crystalline structure, optical and electrical properties have been analyzed as a function of the dopant ion and of the annealing temperature.

## **2. Experimental**

Transparent ZnO thin films have been grown on glass substrates in an Alcatel SCM 650 sputtering system, within a mixture of O<sub>2</sub> and Ar gases (relative oxygen fraction of 0.23), at a constant working pressure of 0.7 Pa, under 50°C and at a deposition rate of 2 nm/min. The target consisted of a hyper-pure (99.99%) metal zinc wafer spaced 60 mm away from the substrates. Radio frequency (13.56 MHz) reactive sputter deposition has been carried out after the camera has reached a base pressure of  $5 \times 10^{-5}$  Pa.

The non-doped, both the as-grown and the 500°C-annealed samples, have been analyzed by Raman spectroscopy, X-ray photoelectron spectroscopy (XPS), X-ray diffraction, transmittance and d.c conductivity techniques. Afterwards, the as-grown films were

implanted with Sb, Al and P ions with a fluence of  $5 \times 10^{15}$  atm/cm<sup>2</sup> and energy of 150 KeV for Sb and 100 KeV for the other two ions. In order to recover from the implantation damage and to activate the implanted ions, samples have been annealed for 60 min, in vacuum, either at 300°C or at 500°C.

The micro-structure of thus resulting films has been analysed by X-ray diffraction and Raman scattering. XPS analysis of some specific samples has been performed as well. Films thickness and optical parameters have been determined by optical transmittance in the visible and near IR range from 300 to 2500 nm. Electrical dark conductivity,  $\sigma_d$ , has been measured from 25°C to 95°C, using thermally evaporated coplanar Al contacts with an electrode gap of 1.0 mm under a typical applied voltage of 0.1 Vd.c.

X-ray experiments have been performed at room temperature in a Siemens D5000 diffractometer using Cu-K $\alpha$  radiation, in a Bragg-Bretano geometry in the range  $10^\circ < 2\theta < 80^\circ$ . Micro-Raman spectra have been measured in a frequency range of 200-700 cm<sup>-1</sup>, using the 514.5 nm excitation line of an Ar<sup>+</sup> laser, in the back scattering geometry, on a Jobin-Yvon T64000 spectrometer equipped with a liquid nitrogen cooled CCD detector. In order to avoid heating the sample, the incident power has been kept at 20 mW. XPS measurements have been carried out under monochromatic Al-K $\alpha$  radiation ( $h\nu = 1486.92$  eV) using a VG Escalab 250 iXL ESCA instrument (VG Scientific). Optical transmittance spectra of the films have been acquired in a Shimadzu UV 3101 PC spectrophotometer.

### **3. Results and discussion**

The X-ray diffraction spectra of all ZnO thin films, non-doped and annealed-doped, reveal the existence of a single phase hexagonal wurtzite structure as in bulk ZnO. Only

(002) and (004) peaks have been observed in all the films due to their highly crystalline preferential orientation along the c-axis, perpendicular to the substrate surface.

Figure 1 shows XRD spectra of a typical ZnO thin film exhibiting (002) peak, before implantation (as-grown and 500°C-annealed) and after implantation (annealed at 300°C and 500°C). The FWHM of the (002)-peak is larger in both implanted-300°C/500°C-annealed samples than in the annealed non-implanted one. This trend has been observed in all doped samples and indicates that the crystalline structure has been partially damaged by implantation. Furthermore, a displacement towards bigger  $2\theta$  of the (002)-peak position has been observed for increasing annealing temperature, over-crossing the ZnO bulk value ( $2\theta_{\text{bulk}} = 34.44^\circ$ ) in most cases. As we have already reported, in the case of the non-doped samples the temperature annealing releases the compressive stress within the films <sup>[7]</sup>. The present results show that for the doped samples the annealing treatment not only releases the compressive stress but also induces a slightly tensile one (see Table I).

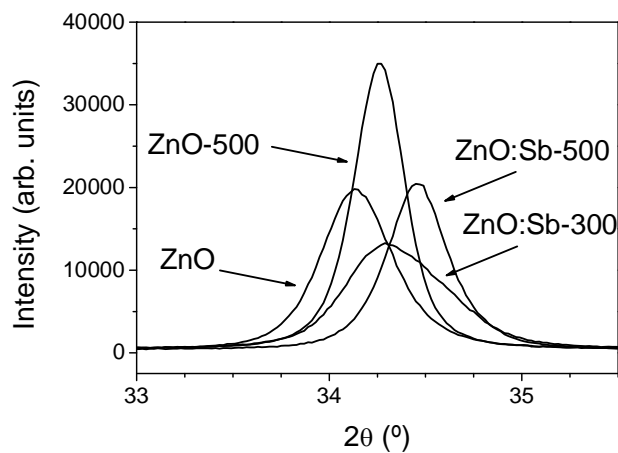


Figure 1 –XRD spectra of a typical ZnO thin film exhibiting (002) peak, before implantation (as-grown and annealed) and after implantation (annealed at 300°C and 500°C).

Structural parameters obtained from X-ray diffraction analysis are shown in Table I. The average crystal size <sup>[8]</sup> of the implanted-500°C-annealed films is lower than the crystal size obtained for the non-doped samples, annealed at the same temperature.

Table I - Structural parameters obtained by XRD and Raman scattering

Sample	Annealing temperature	from XRD		from Raman	
		D <sub>x</sub> (nm)	σ (GPa)	ω <sub>R</sub> (cm <sup>-1</sup> )	FWHM (cm <sup>-1</sup> )
ZnO	as-grown	16.5	-3.08	440.2	16.9
ZnO-500	500°C	24.6	-1.51	439.1	9.6
ZnO:P-300	300°C	13.3	-0.11	438.7	13.5
ZnO:P-500	500°C	19.1	0.77	438.2	10.3
ZnO:Sb-300	300°C	8.8	-0.42	438.6	16.5
ZnO:Sb-500	500°C	21.3	1.01	438.5	10.4
ZnO:Al-300	300°C	16.0	1.22	438.4	12.8
ZnO:Al-500	500°C	21.3	1.39	437.7	11.6

Vibrational properties of the ZnO thin films have been studied by Raman spectroscopy. c-ZnO phonon modes are the E<sub>2</sub> at 101 cm<sup>-1</sup> and at 437 cm<sup>-1</sup>, the A<sub>1</sub> and E<sub>1</sub> transverse modes at 380 cm<sup>-1</sup> and 407 cm<sup>-1</sup>, respectively, and the longitudinal modes (LO) at 574 cm<sup>-1</sup> and 583 cm<sup>-1</sup>[9].

Figure 2-a) depicts the Raman spectra of the Sb implanted ZnO films, after annealing. These spectra show both the usual peak at about 437 cm<sup>-1</sup> assigned to the non-polar optical phonons (E<sub>2</sub>-high) mode and a band between 500 and 650 cm<sup>-1</sup> centered at

$\approx 575 \text{ cm}^{-1}$ . This band seems to result from the superposition of three contributions: the two LO modes predicted for c-ZnO and a contribution at  $595 \text{ cm}^{-1}$  assigned to the  $E_1$  (LO) mode related to defects of O-vacancy and Zn interstitial <sup>[10, 11]</sup>. With the increasing of the annealing temperature, the intensity of the  $E_2$  mode frarily increases, its peak position shifts towards the bulk ( $437 \text{ cm}^{-1}$ ) position <sup>[12]</sup> and its FWHM decreases (see Table I and Fig. 2-a). By the contrary, the intensity of the  $575 \text{ cm}^{-1}$  band strongly diminishes which can be related to the recovering of the oxygen bonds during thermal treatment.

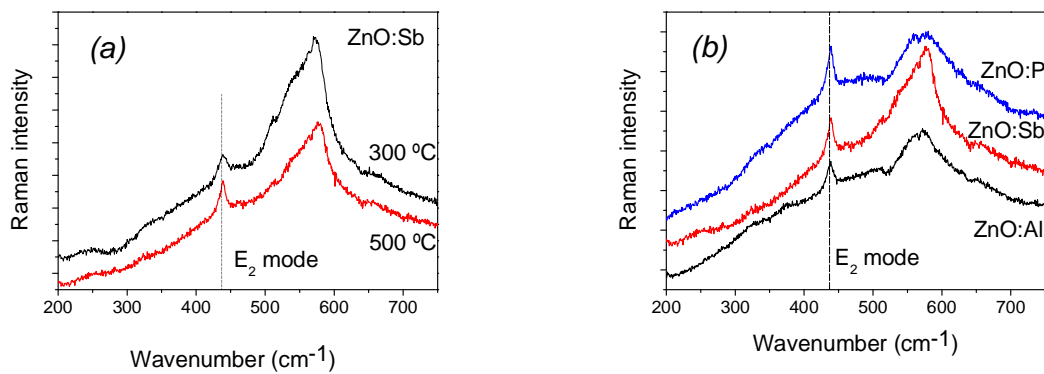


Figure 2 – (a) Raman spectra of ZnO:Sb thin film annealed at 300°C and at 500 °C; (b) Raman spectra of P, Sb, and Al-doped-500°C-annealed films.

Raman spectra of all doped-500°C-annealed films are shown on Fig 2-b). The spectra shape is approximately the same, despite the dopant. However, for the ZnO:Sb the relative importance of the  $575 \text{ cm}^{-1}$  band is much bigger than the  $E_2$  mode.

XPS analysis have provided information about the dopant-O bonds in both 300°C and 500°C annealed films. As it can be seen in Fig. 3, the amount of dopant-O bonded clearly increases from 300°C to 500°C-annealed samples. We may thus infer that more doping

ions are effectively incorporated substitutionally at zinc sites in ZnO lattice. A higher temperature treatment also promotes a more uniform dopant depth distribution.

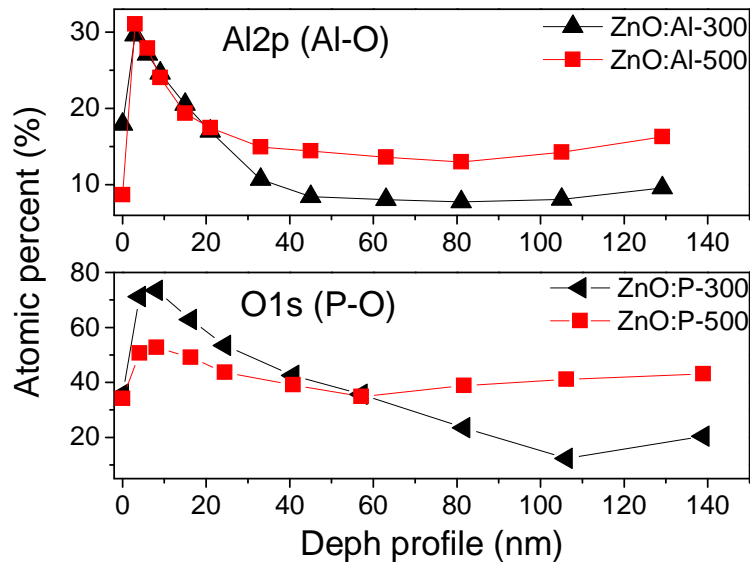


Figure 3 – Atomic percentage of the dopant-O bonds (P-O and Al-O) versus depth profile, for the 300°C and 500°C annealing temperature

All the films (both doped and non-doped) are highly transparent in the visible and near IR range, as it can be seen in Fig. 4, where the experimental spectra of ZnO:Al annealed at 300°C (Fig. 4-a) and at 500°C (Fig. 4-b), and the corresponding fits are shown. By fitting spectra, thickness and optical parameters of the films have been determined using the Minkov method <sup>[13]</sup> and adopting the unified treatment of Forouhi and Bloomer <sup>[14]</sup> for the dispersion behavior of the dielectric constant. As it can be seen in Fig 4-b, Al-doped samples annealed at 500°C show a free-electron contribution to its transmittance spectrum (though ignored in the simulation), well seen at wavelengths higher than 1800 nm. This behavior is in agreement with the difference in resistivity ( $\rho$ ) values between

300°C and 500°C-annealed-Al-doped samples (see Table II). Transmittance spectra of just-implanted samples denotes significant diffusion at wavelengths lower than 800nm. Under 300°C-thermal-treatment this diffusion contribution is much weaker through slightly bigger than in the 500°C-annealed case (Table II). The diffusion decreasing from non-annealed to 300°C-annealed films occurs possibly because during the 300°C annealing a part of the implanted ions migrate into substitutional Zn-sites. On the other hand, the higher temperature annealing may lead to the segregation of non-incorporated dopant ions onto grain-boundary, resulting in more intense optical diffusion.

In a previous work we have already mentioned that the refractive index of non-annealed ZnO thin films was higher than its bulk value, although after annealing it decreased to a slightly below bulk value <sup>[7]</sup>. We have related this effect to the presence of stress in the as-grown films. A similar effect is observed in all implanted films. Before annealing the refractive index is higher than the bulk value, decreases after annealing at 300°C and decrease again after 500°C-treatment, reaching a value lower than the bulk, as it can be seen in Table II.

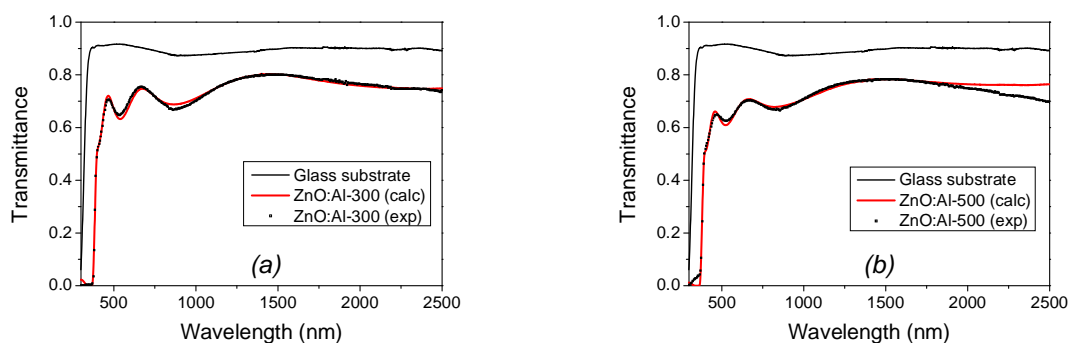


Figure 4 – Experimental transmission spectra and the corresponding fits, for: (a) ZnO:Al annealed at 300°C; (b) ZnO:Al annealed at 500°C



Table II – Optical and electrical parameters

Sample	Film thickness (nm)	Optical parameters		Electrical parameters	
		$n_{(633)}$	$k_{\text{dif}(633)}$	$\rho_{\text{RT}} (\Omega\text{cm})$	$E_{\text{act}} (\text{eV})$
ZnO		2.038	–	$2 \times 10^8$	0.78
ZnO-500		2.008	–	$1.8 \times 10^8$	0.77
ZnO:P	377	2.050	$3.11 \times 10^{-3}$	–	–
ZnO:P-300	365	2.020	$0.62 \times 10^{-3}$	$3.74 \times 10^4$	0.397
ZnO:P-500	422	1.880	$1.99 \times 10^{-3}$	0.092	0.019
ZnO:Sb	364	2.084	$3.74 \times 10^{-3}$	–	–
ZnO:Sb-300	379	2.067	$0.93 \times 10^{-3}$	13.6	0.064
ZnO:Sb-500	354	1.981	$2.77 \times 10^{-3}$	1.77	0.052
ZnO:Al	349	2.024	$6.66 \times 10^{-3}$	–	–
ZnO:Al-300	332	2.014	$5.17 \times 10^{-3}$	739.1	0.169
ZnO:Al-500	338	1.924	$6.11 \times 10^{-3}$	0.097	0.020

In order to calculate the activation energy and the resistivity of the films, dark current measurements have been performed as a function of temperature. These results are shown in Table II. Resistivity and activation energy strongly decrease with the increase of the annealing temperature. After annealing at 500°C, all doped films exhibit resistivity lower than 0.1  $\Omega\text{cm}$  for Al and P-doped samples and around 1.8  $\Omega\text{cm}$  for Sb-doped film. Before implantation, resistivity values were at least 6 orders greater.

These results can be explained: as it is corroborated by the XPS results, the high-temperature-annealed films have more doping ions effectively incorporated substitutionally in ZnO lattice, which increases the carrier concentration. By the other hand, after the thermal treatment higher crystallization has been achieved, increasing the mobility of the carriers.

#### **4. Conclusions**

Non-doped ZnO thin films have been synthesized by reactive magnetron r.f. sputtering after which Al, or P, or Sb-doping has been achieved by implantation. All the films are polycrystalline with hexagonal structure and a preferred orientation along the c-axes, perpendicular to the substrate. Damage implantation is partially recovered by annealing at 300°C and 500°C.

The annealing has resulted in a significant increase of the electrical conductivity of the films by increasing both the carrier concentration and their mobility, as stated by crossing the XPS and XRD with electrical results.

Though doping introduces optical diffusion, high optical transmittance of the films (> 0.7-0.8) is maintained. From doped-non-annealed to doped-300°C-annealed films this diffusion effect greatly decreases but it slightly increases from 300°C to 500°C doped-annealed films. The former behavior can be explained due to the incorporation of the ion dopant into substitutional Zn-sites and the latter to the non-incorporated dopant ions that are segregated onto grain-boundary.

Thus, structural, optical and electrical properties of the doped ZnO films proved to be better improved by thermal treatment at 500°C. The films so obtained are highly

conductive and transparent in the visible and near IR range, which makes this material a good candidate for the desired optoelectronic applications.

**References:**

- [1] Zhang Xiaodan, Fan Hongbing, Zhao Ying, Sun Jian, Wei Changchun, Zhang Cunshan, *Appl. Surface Science* 253, 3825 (2007)
- [2] T.M. Børsetha, J.S. Christensena, K. Maknysa, A. Hallénb, B.G. Svenssona, A.Yu. Kuznetsova, *Superlattices and Microstructure* 38, 464 (2005)
- [3] V. A. Coleman, H. H. Tan, C. Jagadish, S. O. Kucheyev, J. Zou, *Appl. Phys. Lett.* 87, 231912 (2005)
- [4] Yasemin Caglar, Saliha Ilican, Mujdat Caglar, Fahrettin Yakuphanoglu, *Spectrochimica Acta Part A Molecular and Biomolecular Spectroscopy* (2006) available on line at science direct.com
- [5] J. Lee, J. Metson, P.J. Evans, R. Kinsey, D. Bhattacharyya, *Appl. Surface Science* 253, 4317 (2007)
- [6] Haiyan Wang, Xiaoyong Gao, Qiliang Duan, Jingxiao Lu, *Thin Solid Films* 492, 236 (2005)
- [7] A.G. Rolo, J. Ayres de Campos, T. Viseu, T. de Lacerda-Arôso, M.F. Cerqueira, *Superlattices and Microstructure* in print (2007)
- [8] Th.H. de Keijser, J.I. Langford, E.F. Mittermeyer, A.B.P. Rogels, *J. Appl. Crystallogr.* 11, 10 (1978)
- [9] C. Bundesmann, N. Ashkenov, M. Schubert, D. Spemann, T. Butz, E. M. Kaidashev, M. Lorenz, and M. Grundmann, *Appl. Phys. Lett.* 83 (10), 1974 (2003)

- [10] T.C. Damen, S.P.S. Porto, B. Tell, Phys. Rev. 142(2), 570 (1966)
- [11] J.M. Calleja, M. Cardona, Phys. Rev. B 16, 3753 (1977)
- [12] B.H. Bairamov, A. Heinrich, G. Irmer, V.V. Toporov, E. Ziegler, Phys. Status Solidi B 119, 227 (1983)
- [13] D.A. Minkov, J. Phys D: Appl. Phys. 22, 199 (1989)
- [14] A.R. Forouhi, I. Bloomer, Phys. Rev. B 34, 7018 (1986)